JTTEE5 17:858–864
DOI: 10.1007/s11666-008-9251-8
1059-9630/$19.00 © ASM International

TGO Growth and Crack Propagation in a Thermal Barrier Coating

W.R. Chen, R. Archer, X. Huang, and B.R. Marple

(Submitted May 8, 2008; in revised form September 22, 2008)

In thermal barrier coating (TBC) systems, a continuous alumina layer developed at the ceramic topcoat/bond coat interface helps to protect the metallic bond coat from further oxidation and improve the durability of the TBC system under service conditions. However, other oxides such as spinel and nickel oxide, formed in the oxidizing environment, are believed to be detrimental to TBC durability during service at high temperatures. It was shown that in an air-plasma-sprayed (APS) TBC system, postspraying heat treatments in low-pressure oxygen environments could suppress the formation of the detrimental oxides by promoting the formation of an alumina layer at the ceramic topcoat/bond coat interface, leading to an improved TBC durability. This work presents the influence of postspraying heat treatments in low-pressure oxygen environments on the oxidation behavior and durability of a thermally sprayed TBC system with high-velocity oxy-fuel (HVOF)-produced Co-32Ni-21Cr-8Al-0.5Y (wt.%) bond coat. Oxidation behavior of the TBCs is evaluated by examining their microstructural evolution, growth kinetics of the thermally grown oxide (TGO) layers, and crack propagation during low-frequency thermal cycling at 1050 °C. The relationship between the TGO growth and crack propagation will also be discussed.

Keywords crack propagation, HVOF, TBC, TGO growth

1. Introduction

The metallic bond coat (BC) is an important constituent of thermally sprayed TBC systems. It enhances the adhesion of the ceramic thermal barrier layer (the topcoat or TC) to the substrate and also provides oxidation and corrosion protection to the substrate metal. At elevated temperatures, however, oxidation of the bond coat results in the formation of a TGO layer at the ceramic/bond coat interface. If the TGO was composed of a continuous scale of Al_2O_3, it would act as a diffusion barrier during an extended thermal exposure in service, thus helping to protect the substrate from further oxidation and improving the durability of the system under service conditions. However, it has been reported that some other oxides, such as chromia $(Cr,Al)_2O_3$, spinel $Ni(Cr,Al)_2O_4$, and nickel oxide NiO (Ref 1-6), may form along with this TGO layer in thermally sprayed TBC systems. Since oxidation of the bond coat has been recognized as the cause for separation of the ceramic layer from the substrate (Ref 2, 3, 7-10), the formation of the detrimental oxides may accelerate crack nucleation during thermal exposure, leading to premature TBC failure. Studies have shown that, when heat treated in low-pressure oxygen conditions, a continuous Al_2O_3 layer may develop at the ceramic/bond coat interface in both thermally sprayed (Ref 6, 11-13) and electron beam physical vapor deposited (EB-PVD) TBC systems (Ref 14-18). Therefore, appropriate postspraying heat treatment(s) may suppress the formation of detrimental oxides by developing a TGO composed of a predominantly Al_2O_3 layer, leading to improved TBC durability.

In the present investigation, heat treatments in environments with low-pressure oxygen were performed to produce an Al_2O_3 layer at the interface between the ceramic topcoat and the bond coat prior to prolonged thermal exposure in air. The influence of the preoxidation treatments on oxidation behavior was then studied in terms of TGO growth, crack nucleation, and propagation in the TBC system having an HVOF-produced bond coat.

2. Experimental

The TBC samples consisted of a CoNiCrAlY bond coat and a ZrO_2-8wt.%Y_2O_3 topcoat. The bond coat was deposited to a thickness of 140 to 180 μm by the HVOF

This article is an invited paper selected from presentations at the 2008 International Thermal Spray Conference and has been expanded from the original presentation. It is simultaneously published in *Thermal Spray Crossing Borders, Proceedings of the 2008 International Thermal Spray Conference*, Maastricht, The Netherlands, June 2-4, 2008, Basil R. Marple, Margaret M. Hyland, Yuk-Chiu Lau, Chang-Jiu Li, Rogerio S. Lima, and Ghislain Montavon, Ed., ASM International, Materials Park, OH, 2008.

W.R. Chen, Institute for Aerospace Research, SMPL, National Research Council Canada, Ottawa, ON, Canada K1A 0R6; **R. Archer** and **X. Huang**, Department of Mechanical and Aerospace Engineering, Carleton University, Ottawa, ON, Canada K1S 5B6; and **B.R. Marple**, Industrial Materials Institute, National Research Council Canada, Boucherville QC, Canada J4B 6Y4. Contact e-mail: Weijie.Chen@nrc-cnrc.gc.ca.

technique (Tafa JP5000, Praxair, CT, USA), with powders of Co-32Ni-21Cr-8Al-0.5Y (wt.%) (CO-210-24, Praxair, CT, USA), onto ∅16 × 10 mm Inconel 625 disks. On top of the CoNiCrAlY, the topcoat was deposited to a thickness of 250 to 280 μm by the APS technique (F4, Sulzer Metco, Westbury, NY, USA), with powders of ZrO_2-8wt.%Y_2O_3 (Metco 204NS, Sulzer Metco, Westbury, NY, USA). Grit blasting was not applied prior to the deposition of the topcoat. The nominal particle size distributions for the BC and TC powders were 20-45 μm and 11-125 μm, respectively. The BC and TC were produced based on the spray parameters recommended by the manufacturers of the torch and feedstock.

Some of the as-sprayed samples were heat-treated in a vacuum furnace at $<10^{-5}$ torr ($P_{O_2} < 0.00028$ Pa) and 1080 °C for 4 h (vacuum heat treatment or VHT), and some others were heat-treated in a low-pressure oxygen environment of about 2×10^{-3} torr ($P_{O_2} \approx 0.056$ Pa) at 1080 °C for 24 h (low-pressure heat treatment or LPOT). All samples were subsequently subjected to low-frequency thermal cycling in air. The thermal cycle consisted of 10 ~ 15-min ramping, 100-h holding at 1050 °C, and >40-min cooling to the ambient temperature (25 °C). The oxidized samples were sectioned after completion of a predetermined time of thermal exposure between 100 and 2500 h, mounted using epoxy, and mechanically polished. The specimens were then examined using a Philips XL30S FEG scanning electron microscope (SEM) with an energy-dispersive spectrometer (EDS). The area and length of TGO, as well as the crack length in the TBC, were measured using ImageTool software, based on the micrographs taken from the cross sections of the tested samples. TGO area was measured by drawing a polygon along the ceramic/TGO and TGO/bond coat interfaces, while TGO length by drawing a line as short as possible along the TGO. About 20-70 micrographs were taken from each sample for the TGO measurement. The various oxides were identified by SEM-EDS, as $NiAl_2O_4$ contains approximately 13-16 at.% Ni and 27-30 at.% Al, while Al_2O_3 and NiO are very easy to be determined.

3. Results and Discussion

3.1 As-Sprayed and Preoxidized Coating Microstructures

The ceramic topcoat contained porosity and some crack-like discontinuities (Fig. 1a). The maximum dimension of the crack-like discontinuities in the ceramic was in the range of 70 to 100 μm. The CoNiCrAlY bond coat, on the other hand, was rather uniform and contained less porosity compared to the ceramic topcoat. Some porosity also appeared at the topcoat/bond coat interface. SEM/EDS semiquantitative analysis showed that the aluminum concentration in the bond coat at the ceramic/bond coat interface was 13 to 19 at.%. After the VHT and LPOT, a nearly continuous thin Al_2O_3 layer was developed at the original ceramic/bond coat interface (Fig. 1b and c), while the aluminum level in the bond coat remained nearly unchanged within the interface region. Meanwhile, some mixed oxide clusters of chromia, spinel, and nickel oxide (CSN) can also be observed at the ceramic/bond coat interface.

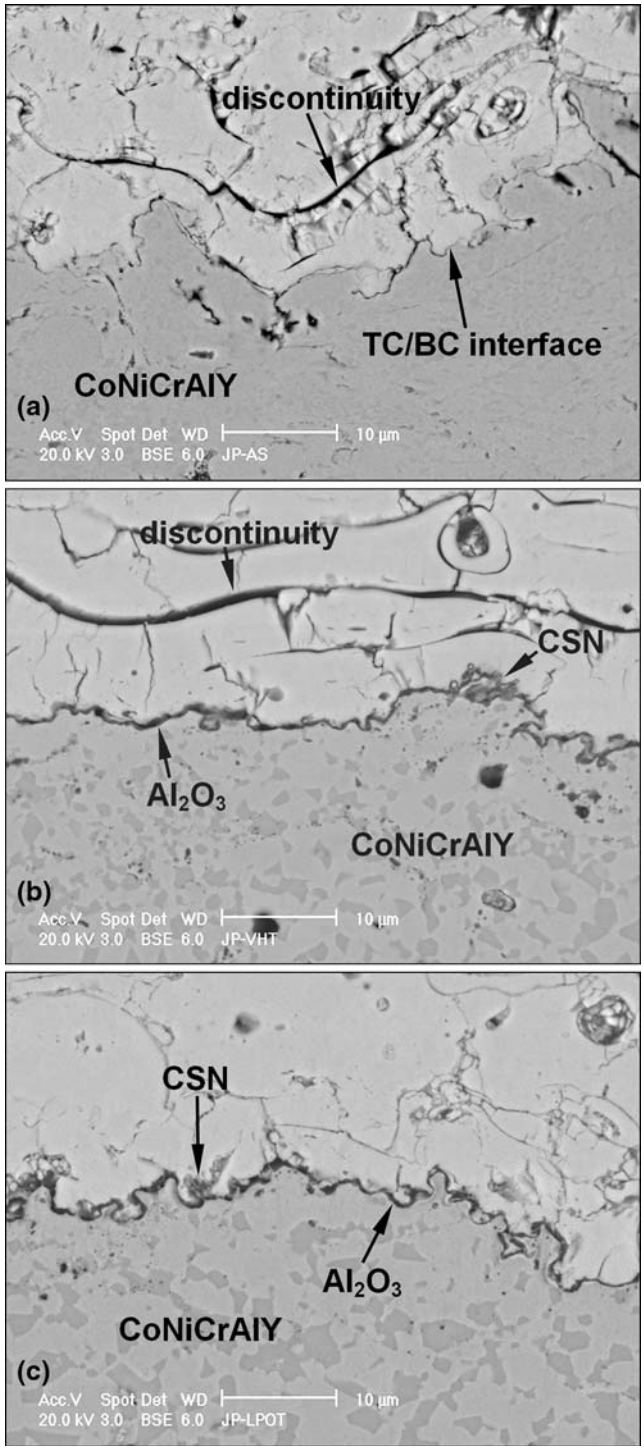

Fig. 1 Microstructures of (a) as-sprayed (i.e., no preoxidation), (b) VHT and (c) LPOT TBCs with HVOF-CoNiCrAlY bond coat

3.2 Oxidation of TBCs

Upon thermal exposure in air, an oxide layer of predominantly Al_2O_3 formed along the interface between the ceramic topcoat and the bond coat (Fig. 2a). In addition, some mixed oxides, CSN clusters, also formed at the ceramic/bond coat interface. The formation of the CSNs was attributed to the localized low aluminum concentration at the ceramic/bond coat interface (Ref 13). As such, the TGO formed in the as-sprayed TBC was composed of an Al_2O_3 layer and a number of CSN clusters. As thermal exposure continued, the TGO layer grew thicker (Fig. 2b). The amount of CSN clusters appeared to be barely changed as exposure time increased, and cracking in the TBC appeared to be very limited.

With a further increase of thermal exposure, preexisting crack-like discontinuities in the ceramic started to open and develop into cracks (Fig. 3a); however, the number of cracks in the TBC was still very limited. Cracking associated with the CSN clusters was also limited, while cracking associated with the TGO occurred mostly at the TGO/bond coat interface (Fig. 3b). Yttrium-rich oxides were observed within the Al_2O_3 as the TGO grew, and the formation of these Y-rich oxides appeared to have no influence on crack nucleation and/or void formation within the TGO. After prolonged thermal exposure, the number of cracks remained limited; however, within 150 μm of the ceramic/bond coat interface, some individual cracks became rather long (Fig. 4), extending up to ~200 μm in length.

In the VHT TBC, however, much less CSNs were formed at the ceramic/bond coat interface (Fig. 5a), compared to those in the as-sprayed TBC (Fig. 2a). This suggests that the VHT could, to a certain level, suppress the formation of mixed oxides during thermal exposure via developing a thin Al_2O_3 layer in vacuum at high temperature. This is consistent with previous observations reported by many other researchers (Ref 6, 11-18). Similar to the as-sprayed TBC, cracking in the VHT TBC was very limited after up to twenty-five 100-h cycles (Fig. 6). The formation of some Cr-rich oxide was observed during

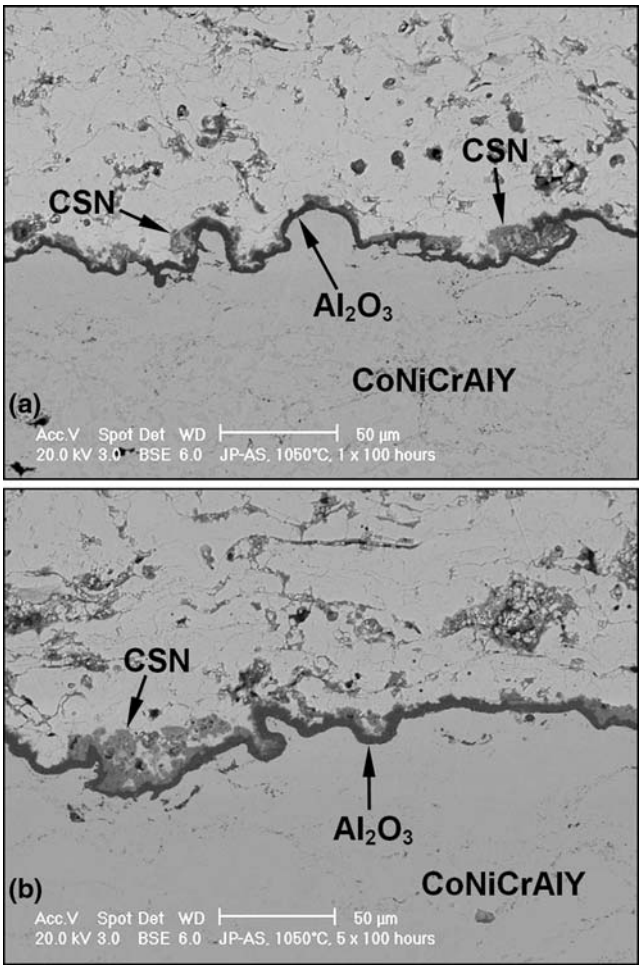

Fig. 2 As-sprayed HVOF-CoNiCrAlY shows (a) a TGO layer of predominantly alumina with CSN clusters between the ceramic topcoat and alumina layer after one 100-h cycle and (b) the increased thickness of the TGO after five 100-h cycles

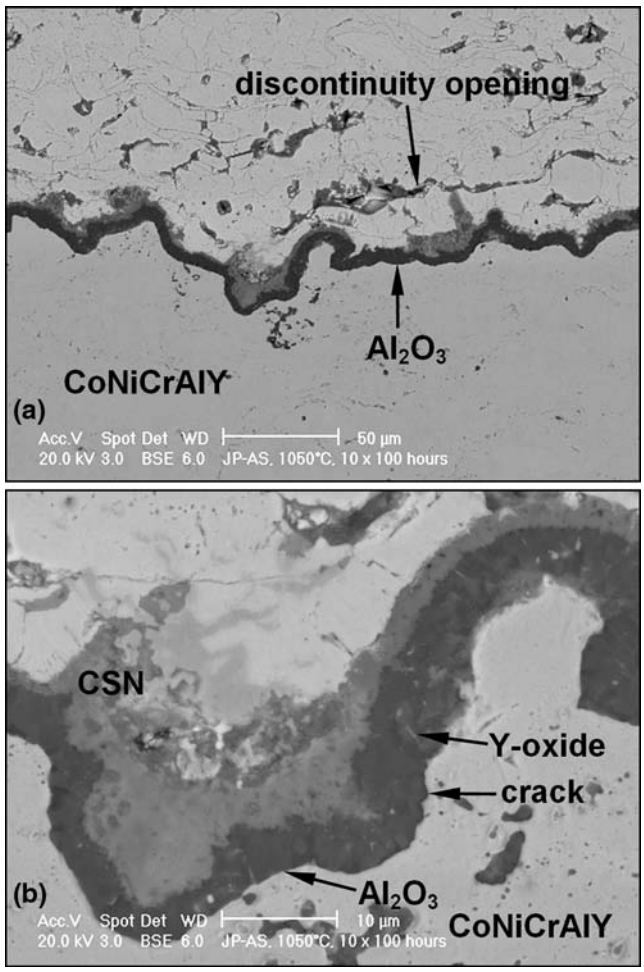

Fig. 3 In the as-sprayed HVOF-CoNiCrAlY, after ten 100-h cycles, a discontinuity in the ceramic/bond coat interface region developed into a crack (a), while cracking associated with the TGO occurred mostly at the TGO/bond coat interface (b)

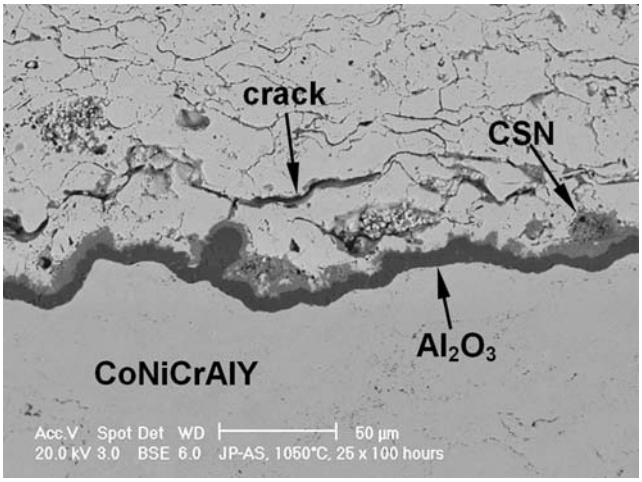

Fig. 4 A discontinuity opened and propagated into a long crack within 100 µm of the ceramic/bond coat interface in the as-sprayed HVOF-CoNiCrAlY after twenty-five 100-h cycles. There are still relatively few cracks in the TBC

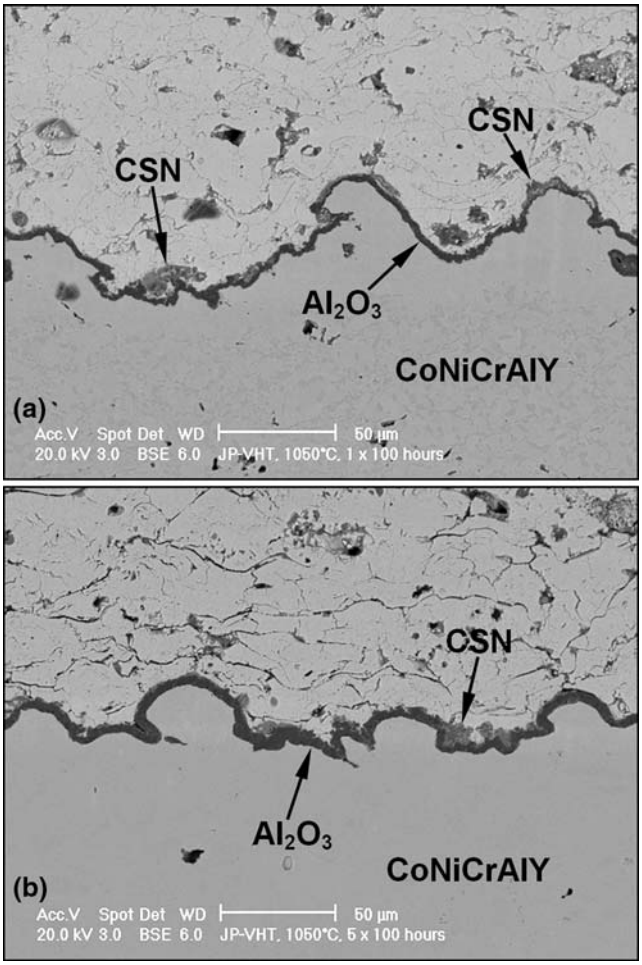

Fig. 5 VHT HVOF-CoNiCrAlY shows (a) a TGO layer of predominantly alumina with limited CSN clusters between the ceramic topcoat and alumina layer after one 100-h cycle and (b) thickening of the TGO after five 100-h cycles

the thickening of the TGO (Fig. 7), where crack nucleation/propagation could be seen. The formation of Cr-rich oxide can be attributed to the aluminum depletion in the bond coat such that a composition was reached at which other oxide(s) could form (Ref 19). The microstructure of the LPOT TBC during thermal exposure was essentially the same as that of the VHT TBC, which had fewer mixed oxides than the as-sprayed TBC, along with a slower TGO thickening process. Cracking associated with mixed oxide clusters at the ceramic/bond coat interface and Cr-rich oxide within the alumina layer could be seen after extended thermal exposure (Fig. 8).

No spallation was observed with any of the three samples (i.e., as-sprayed, VHT, and LPOT) after thirty-five 100-h thermal cycles, and the testing is still in progress.

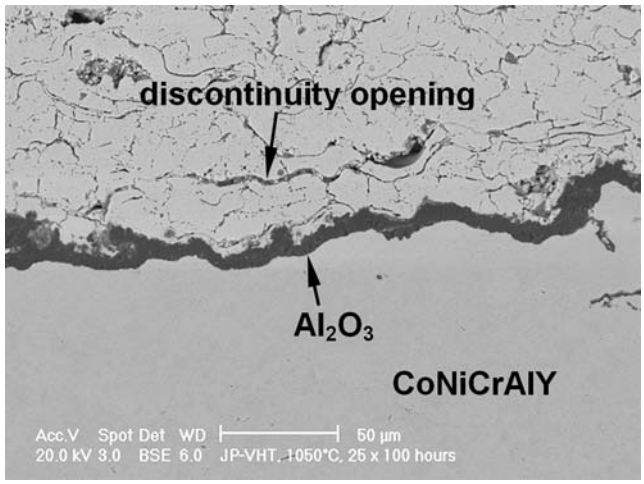

Fig. 6 A discontinuity opened and propagated to become a long crack within 50 µm of the ceramic/bond coat interface in the VHT HVOF-CoNiCrAlY after twenty-five 100-h cycles. Cracking in the TBC remains quite limited

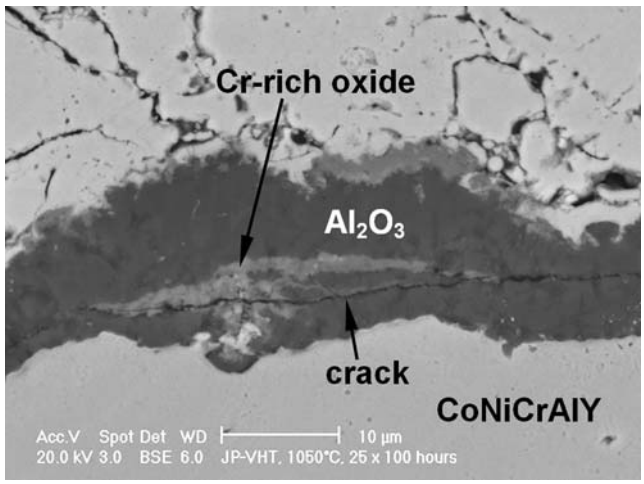

Fig. 7 After twenty-five 100-h cycles, Cr-rich oxide formed during TGO growth, leading to cracking in the VHT HVOF-CoNiCrAlY

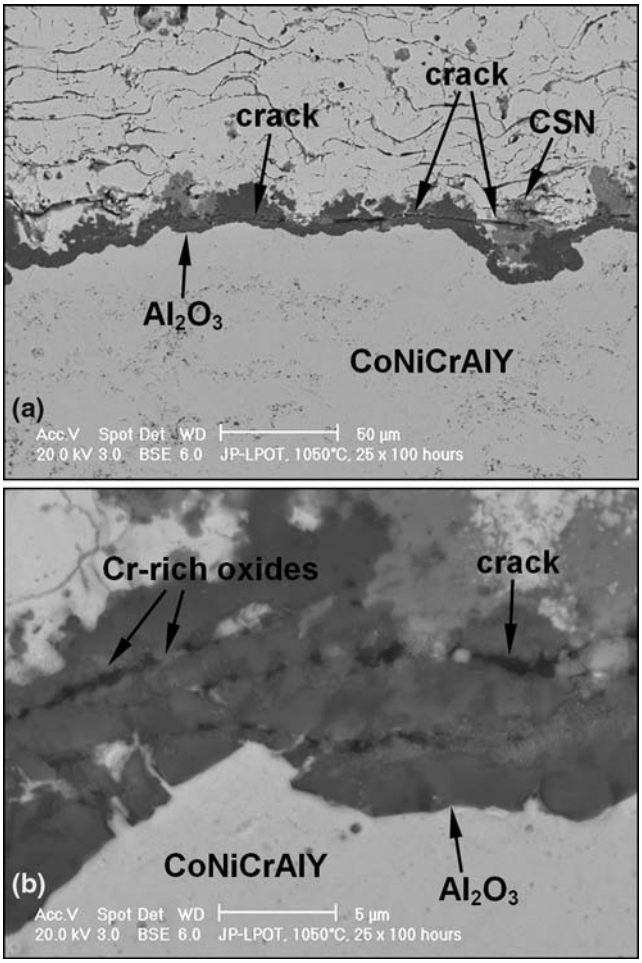

Fig. 8 The LPOT HVOF-CoNiCrAlY TBC coating system after twenty-five 100-h thermal cycles showing (a) cracking associated with CSNs and the alumina layer and (b) cracks nucleated as a result of Cr-rich oxide formation within the alumina layer

3.3 TGO Growth and Crack Propagation in the TBCs

To take into account the entire TGO, an equivalent TGO thickness, δ_{eq}, is defined as (Ref 20):

$$\delta_{eq} = \frac{\Sigma(\text{cross sectional TGO area})}{\Sigma(\text{cross sectional length TC/BC interface})} \quad \text{(Eq 1)}$$

Use of this approach was due to the rough ceramic/bond coat interface, as well as heterogeneous TGO growth especially when CSN clusters were formed between the ceramic topcoat and the bond coat (Fig. 2 and 5). The relationship between δ_{eq}^2 and exposure time (Fig. 9) shows a parabolic growth of TGO, which is consistent with previous observations (Ref 1, 21-23). It can also be seen that both VHT and LPOT can reduce the growth rate of the TGO layer; this can be attributed to the reduced formation of mixed oxides during thermal exposure. However, the difference between the as-sprayed and VHT/LPOT HVOF-CoNiCrAlY is not nearly as pronounced as

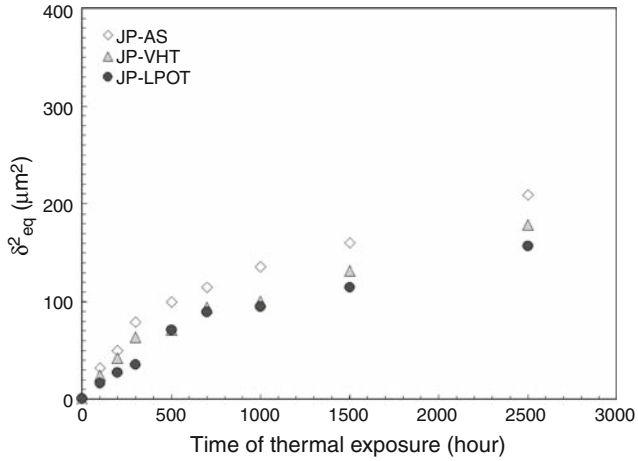

Fig. 9 TGO growth in TBCs with a HVOF-CoNiCrAlY bond coat during low-frequency thermal exposure

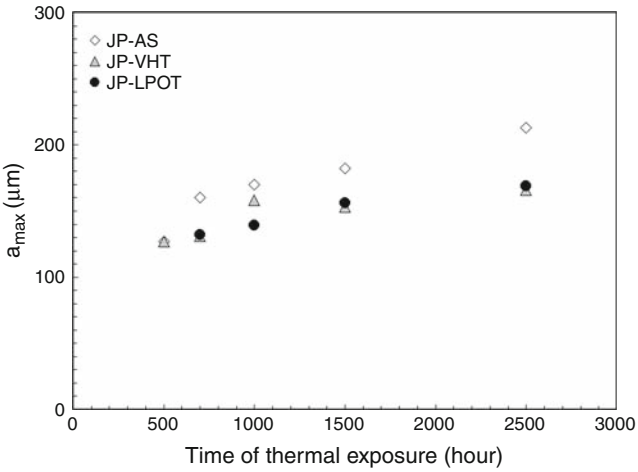

Fig. 10 The maximum crack length in the TBC as a function of the time of thermal exposure

that observed for APS-CoNiCrAlY studied in earlier work (Ref 24). This is due to the smaller amount of the mixed oxides formed in the coating as a result of relatively higher Al content in HVOF-CoNiCrAlY. In the case of APS, oxidation during spraying results in lower Al contents in the deposited CoNiCrAlY coating.

In general, the maximum crack length in the TBCs increased as exposure time increased (Fig. 10). It may be noticed that cracks propagate faster in the as-sprayed TBC than in the VHT and LPOT TBCs. When plotting the maximum crack length as a function of TGO thickness (Fig. 11), it appears that crack length increases with TGO thickness, even though the microstructure of the TGOs varies. Regression analysis shows that the relationship between the maximum crack length in the TBC and TGO thickness can be expressed by a power law, i.e., $a_{max} = k\delta_{eq}^n$, where k and n are constants. The value of n is determined to be 0.891, which is quite different from that

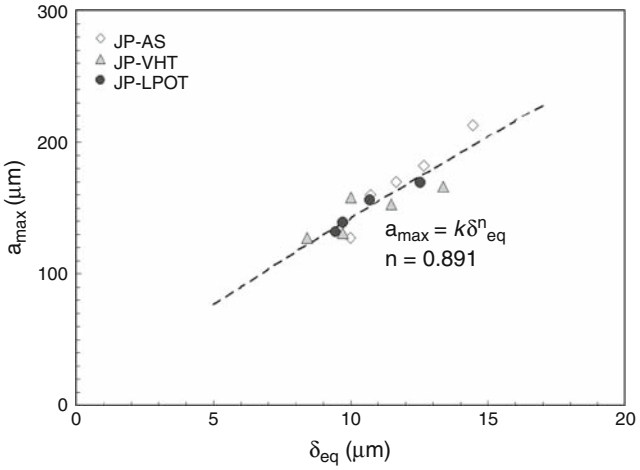

Fig. 11 The maximum crack length in the TBC as a function of TGO thickness

determined in a TBC with an APS-CoNiCrAlY bond coat under a 45-min thermal cycling condition at the same temperature (Ref 24), where n was 0.597. This could be due to the narrow range of TGO thicknesses in the present study, which was from about 8 to 15 μm. Also, the increased holding time in the present study would have an influence on the maximum crack length, since the number of thermal cycles will definitely have an impact on crack propagation. It was reported that longer holding times resulted in a slower mass gain rate during thermal cycling (Ref 25); however, the relationship between holding time and crack length has not been reported in the open literature. Ongoing work by the authors is investigating this relationship.

It has been shown that the critical crack size for initiating TBC spallation is somehow related to the topcoat thickness (Ref 26). It is possible that TBCs with different topcoat thickness values would fail at different TGO thickness levels. As such, determination of TGO growth kinetics, as well as the relationship between crack length and TGO thickness, may be helpful in TBC life prediction. This suggests that the nature of such a relationship merits further investigation in both numerical and experimental studies.

4. Conclusions

The present work investigated the influence of preoxidation treatments in low-pressure oxygen environments on the low-frequency cyclic oxidation behavior of a high-velocity oxy-fuel Co-32Ni-21Cr-8Al-0.5Y (wt.%) bond coat. It was found that both VHT and LPOT could suppress the formation of detrimental mixed oxides to a certain level, and develop a TGO composed of a predominantly Al_2O_3 layer. The growth of the TGO showed a parabolic growth phenomenon up to 2500 h. Crack propagation in the TBC during thermal exposure proceeded via discontinuity opening and growth in the ceramic, as well as limited crack nucleation and propagation associated with the TGO, whereas VHT and LPOT decreased the crack growth rate. A power law relationship between the maximum crack length in the TBC and TGO thickness likely exists, which may be useful to the life prediction of the thermally sprayed TBCs.

Acknowledgments

The authors thank Sylvain Bélanger of the Industrial Materials Institute of NRC Canada for thermal spraying the TBC samples and Peter L'Abbe of the Institute for Chemical Process and Environmental Technology of NRC Canada for preparing the samples for LPOT. They are also grateful to Robert McKellar and Ryan MacNeil of NRC-IAR-SMPL for their help in VHT and oxidation testing. The support from the SURFTEC consortium is also appreciated.

References

1. J.A. Haynes, M.K. Ferber, W.D. Porter, and E.D. Rigney, Characterization of Alumina Scales Formed During Isothermal and Cyclic Oxidation of Plasma-Sprayed TBC Systems at 1150 °C, *Oxid. Met.*, 1999, **52**, p 31-76
2. E.A.G. Shillington and D.R. Clarke, Spalling Failure of a Thermal Barrier Coating Associated with Aluminum Depletion in the Bond-Coat, *Acta Mater.*, 1999, **47**, p 1297-1305
3. A. Rabiei and A.G. Evans, Failure Mechanisms Associated with the Thermally Grown Oxide in Plasma-Sprayed Thermal Barrier Coatings, *Acta Mater.*, 2000, **48**, p 3963-3976
4. C.H. Lee, H.K. Kim, H.S. Choi, and H.S. Ahn, Phase Transformation and Bond Coat Oxidation Behavior of Plasma-Sprayed Zirconia Thermal Barrier Coating, *Surf. Coat. Technol.*, 2000, **124**, p 1-12
5. L. Ajdelsztajn, J.A. Picas, G.E. Kim, F.L. Bastian, J. Schoenung, and V. Provenzano, Oxidation Behavior of HVOF Sprayed Nanocrystalline NiCrAlY Powder, *Mater. Sci. Eng.*, 2002, **A338**, p 33-43
6. W.R. Chen, X. Wu, P.C. Patnaik, and J.-P. Immarigeon, Oxidation Behaviour of a Plasma-Sprayed Thermal Barrier Coating System, *Proceedings from the 1st International Surface Engineering Congress and the 13th IFHTSE Congress* (Columbus, Ohio), 2002, p 535-543
7. R.A. Miller and C.E. Lowell, Failure Mechanisms of Thermal Barrier Coatings Exposed to Elevated Temperatures, *Thin Solid Films*, 1982, **95**, p 265-273
8. C.H. Hsueh, P.F. Becher, E.R. Fuller, S.A. Langer, and W.C. Carter, Surface-Roughness Induced Residual Stresses in Thermal Barrier Coatings: Computer Simulations, *Mater. Sci. Forum*, 1999, **308-311**, p 442-449
9. A.G. Evans, D.R. Mumm, J.W. Hutchinson, G.H. Meier, and F.S. Pettit, Mechanisms Controlling the Durability of Thermal Barrier Coatings, *Prog. Mater. Sci.*, 2001, **46**, p 505-553
10. K.W. Schlichting, N.P. Padture, E.H. Jordan, and M. Gell, Failure Modes in Plasma-Sprayed Thermal Barrier Coatings, *Mater. Sci. Eng.*, 2003, **A342**, p 120-130
11. D. Monceau, F. Crabos, A. Malié, and B. Pieraggi, Effects of Bond-Coat Preoxidation and Surface Finish on Isothermal and Cyclic Oxidation, High Temperature Corrosion and Thermal Shock Resistance of TBC Systems, *Mater. Sci. Forum*, 2001, **369-372**, p 607-614
12. S. Takahashi, M. Yoshiba, and Y. Harada, Failure Analysis of High-Temperature Oxidation for Plasma Sprayed Thermal Barrier Coating Systems with Different Coating Characteristics, *Mater. Sci. Forum*, 2004, **461-464**, p 367-374

13. W.R. Chen, X. Wu, D. Dudzinski, and P.C. Patnaik, Modification of Oxide Layer in Plasma-Sprayed Thermal Barrier Coatings, *Surf. Coat. Technol.*, 2006, **200**, p 5863-5868
14. C. Leyens, K. Fritscher, R. Gehrling, M. Peters, and W.A. Kaysser, Oxide Scale Formation on an MCrAlY Coating in Various H_2-H_2O Atmospheres, *Surf. Coat. Technol.*, 1996, **82**, p 133-144
15. H. Lau, C. Leyens, U. Schulz, and C. Friedrich, Influence of Bondcoat Pre-treatment and Surface Topology on the Lifetime of EB-PVD TBCs, *Surf. Coat. Technol.*, 2003, **165**, p 217-223
16. V.K. Tolpygo and D.R. Clarke, The Effect of Oxidation Pre-Treatment on the Cyclic Life of EB-PVD Thermal Barrier Coatings with Platinum-Aluminide Bond Coats, *Surf. Coat. Technol.*, 2005, **200**, p 1276-1281
17. T.J. Nijdam, L.P.H. Jeurgens, J.H. Chen, and W.G. Sloof, On the Microstructure of the Initial Oxide Grown by Controlled Annealing and Oxidation on a NiCoCrAlY Bond Coating, *Oxid. Met.*, 2005, **64**, p 355-377
18. T.J. Nijdam, G.H. Marijnissen, E. Vergeldt, A.B. Kloosterman, and W.G. Sloof, Development of a Pre-Oxidation Treatment to Improve the Adhesion between Thermal Barrier Coatings and NiCoCrAlY Bond Coatings, *Oxid. Met.*, 2006, **66**, p 269-294
19. F.S. Pettit, Oxidation Mechanisms for Nickel-Aluminum Alloys at Temperatures Between 900 and 1300 °C, *Trans. Metall. Soc. AIME*, 1967, **239**, p 1296-1305
20. W.R. Chen, X. Wu, B.R. Marple, and P.C. Patnaik, The Growth and Influence of Thermally Grown Oxide in a Thermal Barrier Coating, *Surf. Coat. Technol.*, 2006, **201**, p 1074-1079
21. S.M. Meier, D.M. Nissley, and K.D. Sheffler, Thermal Barrier Coating Life Prediction Model Development, ASME 91-GT-40, *International Gas Turbine and Aeroengine Congress and Exposition* (Orlando, FL), 1991
22. W. Brandl, H.J. Grabke, D. Toma, and J. Krüger, The Oxidation Behaviour of Sprayed MCrAlY Coatings, *Surf. Coat. Technol.*, 1996, **86-87**, p 41-47
23. K.S. Chan and N·S. Cheruvu, Degradation Mechanism Characterization and Remaining Life Prediction for NiCoCrAlY Coatings, GT2004-53383, *Proceedings of ASME Turbo Expo 2004, Power for Land, Sea, and Air* (Vienna, Austria), 2004
24. W.R. Chen, X. Wu, B.R. Marple, R.S. Lima, and P.C. Patnaik, Pre-Oxidation and TGO Growth Behaviour of an Air-Plasma-Sprayed Thermal Barrier Coating, *Surf. Coat. Technol.*, 2008, **202**, p 3787-3796
25. Y. Zhang, B.A. Pint, G.W. Garner, K.M. Cooley, and J.A. Haynes, Effect of Cycle Length on the Oxidation Performance of Iron Aluminide Coatings, *Surf. Coat. Technol.*, 2004, **188-189**, p 35-40
26. D. Zhu, S.R. Choi, and R.A. Miller, Development and Thermal Fatigue Testing of Ceramic Thermal Barrier Coatings, *Surf. Coat. Technol.*, 2004, **188-189**, p 146-152